**Introduction**

Phosphotidylinositol-3 kinases (PI3K) are a family of cytoplasmic enzymes integral for cell growth, survival, differentiation and chemotaxis that can be divided into three different classes[1-4]. Members of all three classes phosphorylate the D3 hydroxyl group of the inositol 6 carbon-ring contained in the membrane lipid phosphotidylinositol. This ring is polar and exposed to the cytoplasm, allowing it to serve as a substrate for the production of second messengers required for numerous signalling pathways[5].

Class I PI3K can be divided into subclasses A and B. Class IA consists of isoforms $\alpha$, $\beta$, and $\delta$ and differs from Class IB, isoform $\gamma$, in several ways. Both subclasses consist of a heterodimer formed of a catalytic (p110) and a regulatory (p85, p55, or p50) subunit which associate upon ligation of the upstream receptors specific for each ligand. Phosphorylation of a receptor tyrosine kinase's (RTK) phospho-YXXM motif provides a docking site for association and subsequent activation of Class IA PI3Ks [6, 7]. Until the p110 catalytic subunit associates with one of the regulatory subunits, there is only minimal kinase activity [8].

PI3K-$\gamma$ is activated by members of the $G_i$ protein-coupled receptor ($G_i$PCR) family. Full catalytic activity of PI3K-$\gamma$ requires the formation of a unique trimer consisting of p110$\gamma$ and p101 with the G$\beta\gamma$ of the $G_i$PCR [9]. The p110 catalytic subunits of Class IA and IB differ in a few key amino acid residues that allow them to selectively associate with the appropriate regulatory subunits, while exhibiting minimal cross-reactivity [10]. The p110$\gamma$ subunit is capable of phosphorylating phosphotidylinositol (PtdIns) when not associated with the p101 subunit; however, upon association of the two subunits, p110$\gamma$ changes its substrate specificity to phosphotidylinositol-4,5-bisphosphate

($PtdIns(4,5)P_2$) [11]. Class IA and IB PI3Ks are found in most cells, but Class IB is more prominently expressed in leukocytes, especially macrophages, neutrophils and other cells of myeloid lineage. The role of PI3K-γ in the chemotaxis and directed migration of neutrophils and macrophages to inflammation sites is of key interest currently, and has thus been described as the "cell compass" [12]. PI3K-γ has been shown to be a key mediator of chemoattractant-induced macrophage chemotaxis by C5a, CXCL12, CCL5, CCL2, and CCL22, which all signal through Gi-protein coupled receptors [13,14]. Macrophages lacking PI3K-γ have been shown to exhibit up to a 90% decrease in chemotactic activity *in vivo* [15].

Macrophages and neutrophils lacking PI3K-γ show decreased directionality in response to signals through GiPCRs [14,16], due to its role in directing polymerization machinery to the site of assembly[12]. The ability of a cell to track to the inflammation site depends on the production of an intracellular gradient of $PtdIns(3,4,5)P_3$, or $PIP_3$. Formation of the gradient is dependent on PI3K-γ and the antagonistic phosphatases SHIP (SH2 domain-containing inositol 5-phosphatase) and PTEN (phosphatase and tensin homologue deleted on chromosome ten), D5 and D3 phosphatases respectively [17, 5]. PTEN shows increased localization to the trailing edge of the cell, but is excluded from the lipid raft at the leading edge. PTEN, working in tandem with positive feedback activity by Class IA isoforms at the leading edge provides for further signal amplification [18-21]. The result of this intracellular PIP3 gradient is controlled cytoskeleton rearrangement required for chemotactic activity[15]. In addition, the activity of PI3K-γ in tandem with PI3K-δ catalytic subunits in the cell and the vascular endothelium has been

shown to be a key player in forming the linkages necessary for neutrophil rolling and extravasation at the site of inflammation [22].

The pharmacological regulation of PI3K-γ activity may be a potential target for controlling the damaging effects of inflammatory diseases and autoimmune diseases, mainly by preventing large populations of cells from accumulating in tissues. Due to the high sequence homology of the p110 subunits, it is thought that pharmaceutical targeting of this subunit would not be effective because of cross-reactivity. At this time, the p101 subunit appears to be a much better target because of its unique structural features in addition to its well-defined role in chemotaxis[15].

This study focuses on the role of PI3K-γ in the development of *Leishmania mexicana* infection, the causative agent of New World cutaneous Leishmaniasis. *L. mexicana* causes localized, but chronic lesions in humans, while Old World *L. major* causes localized, self-healing lesions. In most mouse strains, *L. major* and *L. mexicana* infections display lesion progression similar to that found in humans[23]. C57Bl/6 mice display chronic, non-healing lesions upon infection with *L. mexicana*[24], making them an suitable model to study human disease progression and to identify factors that contribute to containment or proliferation of *L. mexicana*.

## Materials and Methods

### Mice

Breeding pairs of PI3K-γ p110 -/- (C57BL/6), generously donated by Dr. Bao Lu (Children's Hospital, Boston, MA), were generated by deletion of ~350 base pairs at the start of exon 2 of the p110-γ gene [25]. This deletion was confirmed by Southern blot analysis of DNA derived from tail clips from all breeding pairs (B. L., et. al, unpublished data). Wild-type (PI3K-γ +/+) C57BL/6 mice were purchased from Harlan (Indianapolis, IN). The experiments were performed using 8- to 10-week-old sex-matched mice in a facility at the Ohio State University according to the guidelines for animal research as required by the National Institutes of Health regulations. Under these guidelines, mice were bred and maintained in ventilated microisolator cages in a specific pathogen-free facility. Any mice showing signs of distress were immediately sacrificed. Animal care facilities at the Ohio State University are fully accredited by the Association for the Assessment and Accreditation of Laboratory Animal Care-International and follow the National Research Council's Guide for the Care and Use of Laboratory Animals.

### Parasites

*L. mexicana* (MNYC/BZ/62/M379) stock cultures were maintained in 129/SVE mice by subcutaneous injection of $5x10^6$ promastigotes into shaven rumps. Parasites for experimental studies were then isolated under aseptic conditions from mice with non-ulcerate lesions that were crushed in a Petri dish containing 5mL supplemented M199 (Gibco, Carlsbad, CA) with 10% Fetal Bovine Serum (FBS) (*Ambogen*, Texarkana, AR), 100U of penicillin/mL and 100μg streptomycin/mL (P/S) (Cambrex, Walkersville, MD)

using a 40μm cell-strainer (Beckton Dickson) and 3-mL syringe plunger (Beckton Dickson). The resulting suspension was then added to tissue culture flasks (Falcon, Franklin Lakes, NJ) containing complete M199 and grown until confluent. A small amount of the confluent parasite solution was then added to flasks containing fresh, supplemented M199. This procedure was continued until the parasites had been subjected to 3-6 passages, resulting in metacyclic promastigotes for use in experiments. New *in vivo* cultures were then begun with metacyclic promastigotes as described above.

**Infection protocols.**

*L. mexicana* promastigotes derived from passage 3-6 were centrifuged at 3000 rpm for 10 minutes, supernatants were then decanted and the parasites were resuspended in supplemented, fresh M199. A 1:5 dilution of parasite suspension was then made for counting purposes, using 10% formalin as the diluent. The quantity of parasites in the initial solution was determined by counting the number of parasites present using an improved Neubauer hemacytometer. Parasites were adjusted to 1-2x$10^8$/mL and peanut agglutinin (PNA, Sigma) was added at 10μg/mL and incubated at room temperature for 15-30 minutes. This suspension was then centrifuged at 200 x g for 10 minutes; purified *L. mexicana* metacyclic promastigotes remained suspended in the solution, while immature or unhealthy parasites precipitated out of solution. The supernatant was then centrifuged at 3000 rpm for 10 minutes and the resulting pellet was washed twice with 50 mL fresh, complete RPMI, then centrifuged as described above each time. The PNA-purified promastigotes were then counted and adjusted to a final concentration of $10^6$ per mL. Mice were anaesthetized using 0.4 mL tribromoethanol (TBE) solution (Sigma), consisting of 0.5g TBE dissolved in 1 mL tert-amyl alcohol (Sigma) and 40 mL distilled

water, injected intraperitoneally. Upon induction of anesthesia, $10^3$ PNA-purified metacyclic promastigotes were injected intradermally using a 30-gauge needle (Becton Dickson) and glass micro-syringe (Hamilton, Reno, NV) in the right ear pinna of each mouse. Sterile PBS, pH 7.4, (Gibco) was then dropped into open eyes to prevent them from drying out while the mice were unconscious. Lesion size was then measured weekly using a dial-gauge micrometer (Mitutoyo, Japan) as determined by subtracting the thickness of the uninfected (control) left ear from the infected right ear.

**Isotype-specific enzyme-linked immunosorbent assay (ELISA).**

Blood was collected at 2, 4, 6, and 8-week time points in 1.5 mL DNAse-, RNAse-free microcentrifuge tubes by tail-clipping *L. mexicana*-infected PI3K-γ -/- and wild-type mice. Blood samples were then refrigerated at 4°C overnight. Upon coagulation, clotted blood was collected and discarded and the remaining plasma was spun at 7000 rpm for 7 minutes to precipitate any remaining debris. The resulting plasma was transferred to a fresh microcentrifuge tube and stored at -20°C. These samples were used to determine titers of *L. mexicana*-specific IgG1 (indicative of a $T_H2$-type response) and IgG2a (indicative of a $T_H1$-type response). Each well of a 96-well flat-bottom microtiter plate (Corning) was coated with 100μL soluble *L. mexicana* antigen (5μg/mL) in PBS (pH 9.0) and incubated overnight at 4°C. Upon removal of the soluble *L. mexicana* antigen from the plate, it was incubated for 2 hours at room temperature with milk blocking solution (5g/100 mL PBS-Tween (PBS-T)). Plates were rinsed, then plasma samples were added in duplicate (starting dilution, 1:100) and serially diluted in PBS-T across the plate, leaving the final well as a blank. Plates were incubated at 37°C for one hour then HRP-conjugated rat anti-mouse $IgG_1$ (1: 5,000 dilution) or HRP-

conjugated rat anti-mouse $IgG_2a$ (1:5,000 dilution) was added in a solution of 25% FBS/75% PBS and incubated for one hour at 37°C. Peroxide substrate (Kirkegaard, Gathersville, MD) was added to the wells and stopped with 5% $H_3PO_4$ solution after 10 minutes. Plates were read on a microplate reader (Molecular Devices, Menlo Park, CA) at 450 nm. Data analysis was conducted using SoftMax Pro software (Molecular Devices).

**Relative parasite dilution assay**

Randomly selected infected ears were removed from sacrificed mice at 3, 6, or 9-week time points. The two layers of skin were then teased apart using tweezers and placed inside-down on a 40μm cell-strainer in a Petri dish containing 5 mL Schneider's Drosophila medium (Gibco) completed with 10% FBS, P/S, and 0.5% 2-mercaptoethanol (2-ME) (Gibco) and were then crushed as described above. The resulting suspension was then centrifuged at 3000 rpm for 10 minutes, the supernatant decanted off, and the pellet resuspended in 400μL complete Schneider's Drosophila medium. Samples were added in duplicate to 96-well tissue culture plates (TPP, Trasadingen, Switzerland) at a 1:10 initial dilution and then serially diluted across the plate. Plates were incubated at 30°C for 96 hours and then read using an inverted microscope. The wells were then examined in series until no promastigotes could be found and the last well containing promastigotes was marked, giving the limiting dilution for each sample in logarithmic form.

**Bone marrow-derived macrophages (BMDM)**

Femurs and tibias from 6-8 week old PI3K-γ -/- and wild-type mice were cleaned and isolated intact. Epiphyses from both ends were removed with scissors in a tissue culture hood and the marrow was removed by inserting a needle into the cavity and

rinsing with PBS, pH 7.4, until no marrow remained. This suspension was centrifuged at 1550 rpm for 10 minutes and the erythrocytes contained in the resulting pellet were resuspended and lysed with 5 mL ACK lysis buffer (150mM $NH_4Cl$, 10mM $KHCO_3$, $Na_2EDTA$ 100μM) for 3 minutes and then diluted to 50 mL with complete RPMI (10% FBS, P/S, 0.5% 2-ME). This was centrifuged as described above, the resulting pellet was rinsed twice with complete RPMI, and was resuspended in 25 mL complete RPMI. Living cells were enumerated using Trypan blue (Gibco) exclusion (1:2 dilution) on an improved Neubauer hemacytometer. Cell concentration was adjusted to $10^6$/mL and 10-30x$10^6$ cells plated in 250$cm^2$ tissue culture flasks with vented caps (Corning, Corning, NY). L929 supernatant (10%) cultured in-house was added as the source of CSF-1. Macrophages were grown for 8 days or until confluent, then rinsed twice with warm PBS, pH 7.4, and loosened with a rubber scraper. The presence of mature macrophages was confirmed by flow cytometry, as described below, using CD11b conjugated FITC and F4/80 conjugated PE as markers (BD PharMingen, San Diego, CA).

**Macrophage killing assay**

Round cover slips were placed in 24 well plates (TPP, Trasadingen, Switzerland), and then sterilized by microwaving. Under sterile conditions, 5x$10^5$ BMDM were plated in each well and allowed to adhere for 8 hours at 37°C and 5% $CO_2$. Dead or non-adherent macrophages were removed by rinsing twice with warm PBS, pH 7.4. *L. mexicana* from passage 4 were added at 2.5x$10^6$/mL and incubated 12 hours under conditions described above. Wells were then washed 3 times with warm PBS, pH 7.4, followed by addition of complete RPMI and 100U/mL IFN-γ, 100U/mL IFN-γ and 5 μg/mL LPS, or only complete RPMI (-). Macrophages were then incubated for 12 or 24

hours; at the end of each respective incubation period, supernatant was removed for later analysis, followed by washing of wells three times with warm PBS, pH 7.4. Remaining adherent cells were fixed with methanol (Sigma), rinsed, and stained with Giemsa stain (Gibco) for 25 minutes, followed by rinsing with distilled water. Coverslips were removed, allowed to dry, and then fixed facedown to glass slides using Permount. Uninfected cells, infected cells, and the number of parasites per infected cell were then counted. Supernatants were then analyzed for IL-6, IL-10, Il-12p70, and TNF-α using cytokine-specific ELISA as described under the T-cell proliferation section of materials and methods. Nitric oxide (NO) was quantified using the Griess method.

**Isolation of ear lesion cells**

Five infected ears per group were split as described above. Each half was then floated inside down on complete RPMI containing 10 mM 4-(2-hydroxyethyl)-1-piperazineethanesulfonic acid (HEPES) buffer (Gibco) overnight in a tissue culture incubator. After removing the ears, the tubes were then centrifuged at 1200 rpm for 10 minutes, the pellet resuspended in 0.5 mL PBS, and counted as described above. When an insufficient number of cells were isolated, the ears were then digested with 1mg/mL Collagenase A (Sigma) and 25mM HEPES buffer in supplemented RPMI for 2 hours and crushed as described in the parasite dilution assay. The resulting pellet was then resuspended in a Percoll (Amersham Biosciences, Upsalla, Sweden) gradient consisting of 58.2% Hank's balanced salt solution, 28.4% Percoll, 3.2% 10X PBS and 2.33mg porcine heparin (Sigma) and then spun at 500 x g at room temperature to separate leukocytes from debris. Resulting leukocytes were washed with PBS, pH 7.4, and resuspended in 0.5 mL for counting, as described above.

**Flow cytometric analysis**

Ear lesion cells or BMDM were adjusted to $10^6$/mL then placed on ice with 5μL $F_c$ block (BD Pharmingen) per genotype and incubated for a minimum of 15 minutes. Cells were then stained with FITC, PE, or APC conjugated antibodies and incubated for 45 minutes on ice, while covered with aluminum foil. Cells were then rinsed, resuspended in PBS, centrifuged at 1200 rpm for 5 minutes a total of two times. Samples were then run on a FACSCaliber (Beckton Dickson) along with unstained controls. Due to the limited number of available cells, 5000 events were recorded per tube. Populations were then gated for lymphocytes and granulocytes as appropriate. Analysis was conducted using CellQuestPro Software (Becton Dickson).

**T-cell proliferation assay.**

Mice were sacrificed at time points described above; spleens and lymph nodes draining the site of infection were dissected out immediately under sterile conditions. Lymph nodes and spleens were then crushed as described above. The isolated cells were centrifuged at 1200 rpm for 5 minutes, the supernatant decanted, and the resulting spleen pellet was lysed with Boyle's solution for 5 minutes followed by dilution with 10 mL complete RPMI. The cells were then centrifuged again as described above and rinsed twice with complete RPMI. Lymph node cells were adjusted to $3x10^6$/mL and spleen cells to $5x10^6$/mL then 100μL were plated out in 96-well tissue culture plates (TPP) either with (100μg/mL in complete RPMI) or without (only complete RPMI) soluble *L. mexicana* antigen made as described previously[30]. Cells were incubated under conditions described above for 72 hours, and then supernatants from each individual organ were

pooled for later analysis and stored at -80°C. Cytokine specific ELISAs for IL-4, IL-10, IL-12p70, and IFN-γ were then conducted by coating flat-bottom microtiter plates with rat anti-mouse cytokine antibodies (BD Pharmingen), diluted in binding buffer (0.1M $Na_2HPO4$, pH 9.0) followed by overnight incubation at 4°C. Primary antibodies were then removed without rinsing, blocked for 2 hours using 10% FBS/PBS, followed by addition of samples in duplicate and incubation overnight at 4°C. Samples were removed and wells rinsed 3 times using PBS/Tween (Sigma) and secondary antibody (cytokine specific, biotinylated rat anti-mouse) (BD Pharmingen) and incubated for 2 hours at room temperature. Secondary antibody was removed by washing 4 times, and avidin-conjugated alkaline phosphatase (AKP) (BD Pharmingen) was added, incubated at RT for half an hour, and then washed 5 times. P-nitro-phenol phosphate (PNPP) (1 mg/mL) was dissolved in glycine buffer (pH 10.4), then 100μL was added per well and upon development (A=0.600-1.00), plates were read at 405nm using equipment described above.

**Statistics**

Significant results were calculated using Student's unpaired t-test, with $p<0.05$ considered to be significant.

## Results

### Knockout mice.

As expected, PI3K-γ -/- mice, when compared to wild-type (+/+) B6 mice, were confirmed to have the PI3K-γ p110 subunit gene deletion upon Southern blot analysis from DNA derived from breeding pair tail clips (data not shown).

### PI3K-γ -/- mice develop smaller lesions with lower parasite loads.

Approximately 3 weeks post-infection, both groups of mice began to develop lesions. Wild-type B6 mice had consistently larger lesions than PI3K-γ -/- littermates from initial development at 3 weeks, 0.552mm vs. 2.67mm, and grew continuously through the last measurement at 9 weeks (6.7mm vs. 4.0mm) (Fig. 1). PI3K-γ -/- mice were shown to have significantly (p-values $6.5x10^{-5}$-0.012) smaller lesions over this same time period. Relative parasite dilutions show PI3K-γ -/- mice had slightly, but statistically insignificant (p=0.50), higher average parasite loads at 3 weeks, 1.33 log values vs. 1.21 log values (Fig. 2). At six and nine weeks post-infection, PI3K-γ -/- mice had lower average parasite loads than wild-type mice, both of which were statistically significant.

### Decreased production of *L. mexicana*-specific antibody production by PI3K-γ -/-.

Blood samples from infected mice taken at 4, 8, 10 weeks post-infection were analyzed for *L. mexicana*-specific IgG1 (Fig. 3A) and IgG2a (Fig. 3B). IgG1 titers were barely detectable for both groups at 4 weeks post-infection; however, at 8 weeks post-infection wild-type mice produced detectable levels of IgG1, while PI3K-γ -/- had no detectable serum IgG1. At 10 weeks post-infection, wild-type mice had an 8-fold higher

average titer than PI3K-γ -/- mice. IgG2a titers were barely detectable in wild-type mice and slightly higher in the (-/-) mice, the only time that PI3K-γ -/- mice exhibited higher titers of either antibody isotype compared to wild-type mice. PI3K-γ -/- mice did not show a detectable titer of IgG2a at 8 weeks post-infection, while wild-type mice had an average titer of 500. At 10 weeks post-infection, PI3K-γ -/- mice exhibited a barely detectable average titer, while wild-type mice had an average titer of 2000.

**PI3K-γ -/- T-cells do not produce a distinct $T_H1/T_H2$ cytokine milieu.**

IL-4 production by *L. mexicana*-antigen-stimulated, lymph-node-derived T-cells was consistently higher in PI3K-γ -/- mice at 3, 6, and 9 weeks, but was only statistically significant at 6 weeks (p=.0031) (Fig 4A). IL-10 production (Fig. 4B) showed no consistent pattern, being higher in PI3K-γ -/- derived T-cell supernatants at 3 and 6 weeks, but lower at 9 weeks post-infection. Three and nine week intervals did not exhibit statistically-significant differences (p=0.155 and 0.165, respectively); however, PI3K-γ -/- did exhibit a statistically higher ($p=3.17x10^{-6}$) IL-10 level at six weeks. IL-12 production (Fig. 4C) by both groups of mice did not show a distinctive trend, with wild-type mice producing slightly higher levels at 3 and 9 weeks, but PI3K-γ -/- mice producing a higher level at 6 weeks, none of which were statistically significant. IFN-γ production (Fig. 4D) was almost identical between groups at 3 weeks, slightly elevated in wild-type mice at 6 weeks, but statistically (p=.019) higher in PI3K-γ -/- mice at 9 weeks post-infection.

**BMDM cytokine and nitric oxide production.**

BMDM IL-12 (Fig. 5A) was secreted at similar levels at 12 hours in both groups, but at 24 hours significantly-elevated levels were produced by PI3K-γ -/- BMDMs under

unstimulated and IFN-γ stimulated conditions (p=0.012 and 0.040 respectively). At 24 hours, IFN-γ and IFN-γ/LPS stimulated PI3K-γ -/- BMDMs demonstrated significant increases in IL-12 production (p=0.043 and $3.21x10^{-5}$, respectively).

TNF-α production (Fig. 5B) followed this same trend, with similar, yet insignificant, differences in secretion at 12 hours, followed by significantly higher production by PI3K-γ -/- BMDMs under both stimulated conditions ($p=9.7x10^{-5}$ and 0.027, respectively) at 24 hours compared to wild-type BMDMs.

PI3K-γ -/- BMDMs displayed a similar increase in IL-6 production (Fig. 5C) at 24 hour as well, but not at 12 hours. Only IFN-γ-stimulated PI3K-γ -/- BMDMs displayed a significantly (p=0.034) higher level of IL-6 production at 12 hours. As seen with other cytokines, PI3K-γ -/- BMDMs displayed higher levels of IL-6 production at 24 hours compared to wild-type BMDMs, but only unstimulated and IFN-γ/LPS stimulated conditions yielded significant results (p=0.012 and 0.0070, respectively).

IL-10 production (Fig. 5D) by wild-type BMDMs was slightly higher in cells stimulated with IFN-γ and LPS/IFN-γ at 12 hours and slightly lower than that from PI3K-γ -/- derived BMDM, but only the unstimulated (-) condition exhibited a significant difference (p=0.025); however, significant differences in IL-10 production were seen at 24 hours. PI3K-γ -/- derived BMDMs produced significantly higher levels of IL-10 under unstimulated and IFN-γ stimulated conditions (p=0.0055 and 0.013, respectively).

**PI3K-γ -/- and wild-type mice appear to produce similar levels of nitric oxide.**

Nitric oxide (NO) production did not appear to follow the same trend seen in cytokine production. At 12 and 24 hours post-stimulation (Figs. 6A, 6B), the unstimulated BMDMs of wild-type and PI3K-γ -/- lineage produced similar levels of NO,

both of which were statistically insignificant. Interferon-gamma-stimulated cells also produced similar levels of NO at 12 hours post-stimulation, but at 24 hours post-stimulation, supernatants from wild-type BMDMs had significantly higher ($p=0.041$) NO levels. PI3K-γ -/- BMDMs stimulated with IFN-γ/LPS exhibited higher levels of NO production at 12 and 24 hours post-stimulation than their wild-type counterparts; however, neither was considered to be statistically significant.

**PI3K-γ -/- BMDMs display lower infection rates and parasite loads.**

BMDMs cultured in the presence of 10% L929 supernatant, containing CSF-1, were confirmed to be greater than 86% CD11b and F4/80 positive (data not shown), indicating that the cultured cells were macrophages and appropriate for testing the infection rate and parasite loads of the two lineages under different stimulation conditions.

At 12 hours post-infection, PI3K-γ -/- BMDMs contained a lower average number of parasites per cell than wild-type BMDMs under all three stimulation conditions, but only unstimulated and IFN-γ/LPS stimulated cells had significant killing levels ($p=0.043$ and 0.035, respectively) (Fig. 7B). This trend changed slightly at 24 hours post-stimulation, with PI3K-γ -/- BMDMs containing fewer average numbers of parasites under all three stimulation conditions, but only the parasite loads of unstimulated and IFN-γ stimulated BMDMs were considered significant ($p=0.0069$ and 0.0030, respectively).

The infection rate (Fig. 7A) correlated well with our initial predictions. PI3K-γ -/- BMDMs had consistently lower infection rates under all three conditions at both 12 and 24 hours ($p<0.025$), with one exception. Unstimulated BMDMs at 24 hours

demonstrated a lower average infection rate as well, but this was not significant ($p=0.177$).

**PI3K-γ -/- lesions contain significantly lower macrophage populations.**

Upon flow cytometry analysis, it was determined that no significant difference existed in the composition of the leukocyte populations obtained from ear lesions; however, when the number of cells isolated from each genotype was compared, noticeable differences were discovered. When leukocytes from infected ears taken at 3, 6, and 9 weeks post-infection were enumerated, PI3K-γ -/- lesions consistently yielded lower numbers of cells. Upon further analysis, it was determined that PI3K-γ -/- lesions contained 46.2%, 48.7%, and 54.5% fewer cells compared to their wild-type counterparts at 3, 6, and 9 weeks respectively (Fig. 8).

**Discussion**

Lesion development progressed as expected, with an initial difference between genotypes discernable at 3 weeks post-infection, an incubation time within normal expectations. Given the known deficiencies of PI3K-γ -/- neutrophil and macrophage migration towards the source of C5a, IL-8, as well as fMLP, and numerous chemokines produced at the site of infection [13,14], it was expected that PI3K-γ -/- mice would develop smaller lesions than their wild-type counterparts. It was our hypothesis that depriving the parasites of their obligate host cell, macrophages[26], would lead to a lesser extent of infection; if there are fewer macrophages to present at the infection site, then there are fewer opportunities for the parasite to exploit host macrophages for reproductive purposes, effectively hindering the ability of the parasite to multiply rapidly *in vivo*. The presence of fewer leukocytes at the infection site in PI3K-γ -/- mice explains the smaller lesion size.

Reduced parasite loads at the infection site of PI3K-γ -/- mice also contributed to the smaller lesion size, with the exception of the time points taken at 3 weeks post-infection, where the average parasite load was minimally lower in wild-type mice. Analysis of leukocyte populations in infected ears confirmed previous findings as well as our initial hypothesis, that depriving the parasite of its obligate host cell would reduce the parasite load as well as the lesion size in PI3K-γ -/- mice.

As shown by flow cytometric data, macrophage populations were reduced at the lesion site of PI3K-γ -/- animals, despite the lack of a significant difference in circulating white blood cell counts[22]. With nearly a 50% reduction in the total number of

macrophages at each of the three time points, these data correlate well with previous data describing impaired chemotaxis in PI3K-γ -/- macrophages.

PI3K-γ has been implicated as a potentially necessary factor for B-cell antigen dependent differentiation [27,28]; however, it was not clear whether this defect was due to actual B-cell defects or impaired antigen presentation[15]. Sasaki et al. have shown that PI3K-γ was not required for B-cell development and function[27]; therefore, the decreased serum levels of *L. mexicana*-specific antibodies, both IgG1 and IgG2a, is not attributable to a lack of B-cells or their ability to recognize antigen and respond accordingly. It has been shown that B-cell chemotaxis in response to lymphoid chemokines is not impaired in PI3K-γ -/- animals[29]. Instead, previous groups have hypothesized that the *in vivo* reduction of serum antibody production is due to decreased antigen presentation in secondary lymphoid organs[15].

Migration of antigen-stimulated dendritic cells to regional draining lymph nodes has been shown to be impaired in PI3K-γ -/- cells[30], and it is highly likely that this finding can be extended to the mechanism of macrophage chemotaxis to draining lymph nodes as well. Since macrophages lacking the PI3K-γ gene display decreased migration and directionality when sensing chemokine gradients towards the site of infection, they also are likely to exhibit impaired trafficking to secondary lymphoid organs where antigen presentation to B-cells and helper T-cells occurs. This, paired with the already significant decrease in macrophages at the site of infection provides a convincing explanation as to the reduced Ig production in PI3K-γ mice.

Clearance of *L. mexicana* and other intracellular parasites generally requires the induction of a $T_H1$ immune response, characterized by increased production of IL-12 and

IFN-γ by T-cells[26]. PI3K-γ -/- T-cells isolated from the regional lymph node draining the site of infection did not produce cytokines distinctly indicative of a $T_H1$ response upon stimulation with soluble *L. mexicana* antigen. This observation contrasts with previous research determining PI3K-γ to be a necessary factor for survival and activation of mature T-cells[27]. Surprisingly, IL-4 production by PI3K-γ -/- T-cells was consistently, but not always significantly, higher than that from their wild-type counterparts. IL-4 is associated with reducing the intensity of $T_H1$ responses and shifting it towards a $T_H2$ response, making increased production of this cytokine a susceptibility factor for murine *L. mexicana* infection[23]. A similar trend was also seen with IL-10, which decreases the intensity of $T_H1$ responses as well as downregulating the inflammatory response of macrophages. This decrease in activation is a susceptibility factor for cutaneous *Leishmania* infection as well, due to the necessity of a strong oxidative burst for the macrophage to degrade internalized parasites[26]. Keeping the reduced B-cell response in mind, it was surprising that PI3K-γ -/- T-cells stimulated with *L. mexicana* antigen produced similar, if not higher, cytokine levels compared to their wild-type counterparts, even though wild-type mice did not exhibit impaired antigen presenting cell (APC) trafficking to the site of infection and to secondary lymphoid organs as PI3K-γ -/- mice typically display.

IL-12 and IFN-γ production did not show a distinct trend towards a $T_H1$ response, as would be expected, given the relative resistance to infection of PI3K-γ -/- mice. Instead, there was no significant difference between IL-12 production of PI3K-γ -/- mice and wild-types at any of the three time points; however, IFN-γ production was significantly elevated in wild-type mice at 9 weeks, despite the presence of larger lesions.

Taking into account the unexpected lack of a strong $T_H1$ response, it was concluded that the differences in susceptibility were not T-cell dependent.

The results of the BMDM killing experiment were interesting in their own sense; PI3K-γ -/- BMDMs displayed similar cytokine production levels at 12 hours, but by 24 hours, had produced significantly higher levels of all 4 cytokines measured. At least one mode of inhibition of IL-12 production involves GiPCRs, which transduce signals through PI3K-γ [31]. This particular negative regulation mechanism, in the absence of PI3K-γ, would no longer be functional, explaining the increased production of IL-12 at 12 and 24 hours compared with wild-type BMDMs. IL-12 is capable of upregulating IFN-γ production, which in turn induces the production of TNF-α by macrophages. IFN-γ and TNF-α serves as a potent inductor for production of reactive oxygen species (ROS) which are required for effective clearance of intracellular parasites[32].

The increased production of IL-6 and IL-10 appears to be in response to increased inflammatory cytokine production; IL-6 negatively regulates TNF-α production by macrophages, helping prevent inflammatory responses to pathogens from getting out of control[33]. IL-10 plays an antagonistic role to IFN-γ and TNF-α production as well, by promoting degradation of mRNA for these two cytokines[34]. IL-10 has been shown to have antagonistic effects upon IL-12 production as well[35].

PI3K-γ -/- BMDMs had lower average numbers of parasites per cell as well as average infection rate at 12- and 24-hour time points; visible decreases in the average number of parasites per cell and the infection rate were also present within PI3K-γ -/- BMDM groups at 12 and 24 hours. One of the primary mechanisms of parasite internalization by macrophages is mediated by C3bi on the surface of the parasite. This

event occurs through CR1 and CR3 involvement [26] through Type II phagocytosis, in which a C3bi-opsonized particle sinks through the cell, compared to Type I phagocytosis involving membrane ruffling and pseudopod extension[36]. CR1 signals through a GIPCR, so cells lacking PI3K-γ may have partially-impaired uptake ability, potentially accounting for the decrease in the number of parasites per macrophage as well as the percentage of macrophages infected. The role of PI3K-γ in CR3-mediated Type II phagocytosis is unclear at this point. Type I phagocytosis involving CR3 has been shown to require phosphorylation by the Src kinase Hck[36], creating a docking site necessary for the initiation of Class IA PI3K activity [6, 7].

In conclusion, we have shown that mice lacking the PI3K-γ p110 subunit show decreased lesion size as well as parasite load at the site of infection due to decreased ability of macrophages to locate and migrate to the site of infection. Additionally, BMDMs in the presence of *L. mexicana* metacyclic promastigotes show decreased infection rates as well as lower numbers of parasites per infected cell compared to wild-type-derived cells. PI3K-γ -/- macrophages display increased levels of inflammatory cytokines followed by a corresponding increase in anti-inflammatory cytokines as well as potentially impaired Type II phagocytosis. This situation is an interesting paradox for using PI3K-γ inhibitors to combat tissue destruction in inflammatory-mediated autoimmune diseases. Although there are significantly fewer macrophages at the initial site of infection, the macrophages that do reach the site appear to produce significantly higher levels of tissue-damaging cytokines. Further investigation into this phenomenon is required to understand and develop effective pharmaceutical agents for treating

diseases caused by chronic cell infiltrates without exacerbating the inflammatory response of the target cells.

1. Fry, M.J. 1994. Structure, regulation and function of phosphoinositide 3-kinases. *Biochem. Biophys. Acta* 1226: 237-268.
2. Rameh, L.E. and Cantley, L.C. 1999. The role of phosphoinositide 3-kinase lipid products in cell function. *J. Biol. Chem*. 274: 8347-8350.
3. Fry, M.J. 2001. Phosphoinositide 3-kinase signaling in breast cancer; how big a role might it play? Breast Cancer Reas. 3: 304-312.
4. Katso, R., Okkenhaug, K., Ahmadi, K.,White, S.,Timms, J., and Waterfield, M. D. 2001. Cellular function of phosphoinositide 3-kinases: implications for development, homeostasis and cancer. *Annu. Rev. Cell Dev. Biol*. 17: 615-675.
5. Maehama T., Dixon, J. E. 1998 The tumor suppressor, PTEN/MMAC1, dephosphorylates the lipid second messenger, phosphatidylinositol 3,4,5-trisphosphate. *J. Biol. Chem*. 273: 13375-13378.
6. Vanhaesebroeck, B., Leevers, S. J., Ahmadi, K., Timms, J., Katso, R., et al. 2001. Synthesis and function of 3-phosphorylated inositol lipids. *Annu. Rev. Biochem.*70: 535-602.
7. Songyang, Z. Shoelson, S. E. Chaudhuri, M. Gish, G. Pawson, T., et al. 1993. SH2 domains recognize specific phosphopeptide sequences. *Cell* 72: 767-778.
8. Yu, J. Zhang, Y. McIlroy, J. Rordorf-Nikolic, T. Orr, G. A. et al. 1998. Regulation of the p85/p110 phosphatidylinositol 3'kinase: stabilization and inhibition of the p110alpha catalytic subunit by the p85 regulatory subunit. *Mol. Cell. Biol*. 18: 1379-1387.
9. Stephens, L.R. Eguinoa, A. Erdjument-Bromage H, Lui M, Cooke F, et al. 1997. The G beta gamma sensitivity of a PI3K is dependent upon a tightly associated adaptor, p101. *Cell* 89: 105-114.
10. Krugman S, Hawkins PT, Pryer N Braselmann S. 1999. Characterizing the interactions between the two subunits of the p101/p110gamma phosphoinositide 3-kinase and their role in the activation of this enzyme by G beta gamma subunits. *J. Biol. Chem*. 274:17152-17158.
11. Interleukin-12-mediated resistance to *Trypanosoma cruzi* is dependent on tumor necrosis factor alpha and gamma interferonMaier U, Babich A, Nurnberg B. 1999. Roles of non-catalytic subunits in gbetagamma-induced activation of class I phosphoinositide 3-kinase isoforms beta and gamma. *J. Biol. Chem*. 274: 29311-29317.
12. Rickert P, Weiner OD, Wang F, Bourne HR, Servant G. 2000. Leukocytes navigate by compass: roles of PI3Kgamma and its lipid products. *Trends Cell Biol*. 10:466-473.
13. Hirsch E, Katanaev VL, Garlanda C, Azzolino O, Pirola L, et al. 2000. Central role for G protein-coupled phosphoinositide 3-kinase gamma in inflammation. Science 287:1049-1053.
14. Jones GE, Prigmore E, Calvez R, Hogan C, Dunn GA, et al. 2003. Requirement for PI 3-kinase in macrophage migration to MCP-1 and CSF-1. *Exp. Cell Res*. 290:120-131.
15. Fruman DA and Cantley LC. 2001. Phosphoinositide 3-kinase in immunological systems. *Sem. Immunol*. 14:7-18.

16. Hannigan M, Zhan L, Li Z, Ai Y, Wu D, et al. 2002. Neutrophils lacking phosphoinositide 3-kinase gamma shows loss of directionality during N-formyl-Met-Leu-Phe-induced chemotaxis. *Proc Natl Acad Sci USA* 99:3603-3608.
17. Damen JE, Liu L, Rosten P, Humphries RK, Jefferson AB, et al. 1996. The 145-kDa protein induced to associate with Shc by multiple cytokines is an inositol tetraphosphate and phosphotidylinositol 3,4,5-trisphosphate 5-phosphatase. *Proc. Natl. Acad. Sci. USA*. 93: 1689-1693.
18. Funamoto S, Meili R, Lee S, Parry L, Firtel RA. 2002. Spatial and temporal regulation of 3-phosphoinositides by PI 3-kinases and PTEN mediates chemotaxis. *Cell* 109: 611-623.
19. Iijima M, Devreotes P. 2002. Tumor suppressor PTEN mediates sensing of chemoattractant gradients. Cell 109:599-610.
20. Gomez-Mouton C, Lacalle Ra, Mira B, Jimenez-Barada S, Barber DF, et al. 2004. Dynamic redistribution of raft domains as an organizing platform for signaling during cell chemotaxis. *J. Cell. Biol*. 164:759-768.
21. Niggli V, Keller H. 1997. The phosphotidylinositol 3-kinase inhibitor wortmannin markedly reduces chemotactic peptide-induced locomotion and increases in cytoskeletal actin in human neutrophils. Eur. J. Pharmacol. 335:43-52.
22. *Puri KD, Dogget TA, Huang C, Douangpanya J, Hayflick JS, et al. 2005. The role of endothelial PI3Kgamma activity in neutrophil trafficking.*
23. Stamm LM, Räisänen-Sokolowski A, Okano M, Russel ME, et. al. 1998. *Mice with STAT-6-targeted gene disruption develop a Th1 response and control cutaneous Leishmaniasis.* J. Immunol. 161:6180-6188.
24. Rosas LE, Keiser T, Barbi J, Satoskar AA, et al. 2005. Genetic background influences immune responses and disease outcome of cutaneous L. Mexicana infection in mice. Int. Immunol. 17:1347-1357.
25. Barbier M, Attoub S, Calvez R, Laffargue M, et al. 2001. Weakening link to colorectal cancer? *Nature*. 413:796 only.
26. Alexander J, Satoskar AR, and DG Russel. *Leishmania species: models of intracellular parasitism.* 1999. J Cell Science. 112:2993-3002.
27. Sasaki T, Irie-Sasaki J, Jones RG, Oliveira-dos-Santos AJ, Stanford WL, et al. 2000. Function of PI3Kgamma in thymocyte development, T cell activation, and neutrophil migration. Science 287: 1040-1046.
28. Li Z, Jiang H, Xie W, Zhang Z, Smrcka AV, et al. 2000. Roles of PLC-beta2 and –beta3 and PI3Kgamma in chemoattractant-mediated signal transduction. Science 287: 1046-1049.
29. Reif K, Okkenhaug K, Sasaki T, Penninger JM, Vanhaesebroeck B, et al. 2004. *J. Immunol*. 173: 2236-2240.
30. Del Prete A, Vermi W, Dander E, Otero K, et al. 2004. Defective dendritic cell migration and activation of adaptive immunity in PI3K-γ-deficient mice. *Eur. Mol. Bio. J.* 23:3505-3515.
31. La Sala A, Gadina M, Kelsall BL. 2005. G(i)-protein-dependent inhibition of IL-12 production is mediated by activation of the phosphotidylinositol 3-kinase protein 3 kinase B/Akt pathway and JNK. *J. Immunol*. 175:2994-2999.

32. Hunter CA, Slifer T, Araujo F. 1996. Interleukin-12-mediated resistance to *Trypansoma cruzi* is dependent on tumor necrosis factor alpha and gamma interferon. *Infection and Immunity*. 64:2381-2386.
33. Tian Y, Jochum W, Georgiev P, Moritz W, et al. 2006. Kupffer cell-dependent TNF-alpha signaling mediates injury in the arterialized small-for-size liver transplantation in the mouse. *Proc. Natl. Acad. Sci*. 103:4598-4603.
34. Platzer C, Meisel C, Vogt K, Platzer M, et al. 1995. Up-regulation of monocytic IL-10 by tumor necrosis factor-alpha and camp elevating drugs. *Int. Immunol*. 4:517-523.
35. Wilson EH, Wille-Reece U, Dzierszinski F, Hunter CA. 2005. A critical role for IL-10 in limiting inflammation during toxoplasmosis encephalitis. *J Neuroimmunol.* 165:63-74.
36. Le Cabec V, Carreno S, Moisand A, Bordier C et al. 2002. Complement Receptor 3 (CD11b/CD18) Mediates Type I and Type II Phagocytosis. *J. Immunol*. 15:2003-2009.

**Figure 1.** Lesion size of wild-type (grey line) vs. PI3K-γ -/- (black line) B6 mice upon infection with 1,000 PNA-purified metacyclic promastigotes. Lesion size is based on the difference between the thickness of infected vs. uninfected ears of each individual mouse. Graphs are the average of 3 independent experiments with 5-7 mice taken at intervals of 3, 6, and 9 weeks post-infection (n=21-51, total). Error bars indicate standard error (SE) of the mean for compiled lesion data. *, indicates a p-value of <0.05.

**Figure 2.** Relative parasite loads of wild-type (grey bars) vs. PI3K-γ -/- (black bars) based on limiting dilution assays. Value indicates average number of wells containing visible promastigotes 4-6 days post-euthanasia. Y-axis parasite load values increase logarithmically. Error bars indicate SE of the mean for compiled data from 3 individual experiments with a minimum of two mice taken per interval per genotype and run in duplicate (n=15-25). *, indicates a p-value of <0.05.

**Figure 3.** *L. mexicana* specific antibody production by wild-type (grey bars) and PI3K-γ -/- (black bars) mice at 4, 8, and 10 weeks-post infection. Values represent average titers of IgG1 (Fig. 3A)and IgG2a (Fig. 3B) as determined with isotype-specific ELISA. Each sample was run in duplicate. Error bars indicate SE of the mean for compiled data.

**Figure 4.** Cytokine production of *L. mexicana* antigen-stimulated T-cells taken from regional draining lymph nodes of wild-type (+/+)(grey lines) and PI3K-γ -/- (black lines) mice sacrificed at intervals of 3, 6, and 9-weeks post-infection. Data points represent average cytokine production (pg/mL) of IL-4 (Fig. 4A), IL-10 (Fig.4B), IL-12p70 (Fig. 4C), and IFN-γ (Fig. 4D). At intervals where individual lymph nodes contained too few cells to complete the assay, lymph node contents from each group were pooled and then plated. ELISA analysis of supernatants was conducted in triplicate for each of the four cytokines. Error bars represent SE of the mean for compiled cytokine production of three independent experiments with 5-7 mice per time point. *, indicates a value of <0.05.

**Figure 5.** *L. mexicana*-infected bone marrow-derived macrophage (BMDM) induced production of IL-12p70 (Fig. 5A), TNF-α (Fig. 5B), IL-6 (Fig. 5C), and IL-10 (Fig. 5D) by wild-type (grey lines) and PI3K-γ -/- (black lines) in pg/mL. Supernatants were taken at 12 and 24 hours post-stimulation with only media (-), IFN-γ, or IFN-γ/LPS. Values represent average of 3 independent experiments (n=4-6 each per stimulation type). Error bars representing SE of pooled data. *, indicates p-value of <0.05.

**Figure 6.** BMDM production of nitric oxide (NO), by wild-type (grey bars) and PI3K-γ -/- (black bars) derived cells 12 (Fig. 6A) and 24 (Fig. 6B) hours post-stimulation. Values represent average concentration of NO (μM) from two independent experiments (n=4-6 each, per stimulation type). Samples from each stimulation type of each experiment were pooled to conserve supernatants. Error bars represent SE of combined data. *, indicates p-value of <0.05.

**Figure 7.** BMDM killing assay comparing wild-type (grey bars) vs. PI3K-γ -/- (black bars) percentage of infected BMDM (Fig. 7A) and average number of parasites per BMDM (Fig. 7B) at 12 and 24 hours post-stimulation. Values represent average of two

individual experiments (n=4-5 each, per stimulation type). Error bars represent SE of pooled data. *, indicates p-value <0.05.

**Figure 8.** Percent reduction in PI3K-γ -/- leukocyte populations isolated from infected ears taken at 3, 6, and 9-weeks post-infection. Values represent average of three independent experiments, except 9 weeks, which represents only one. An equal number of wild-type and PI3K-γ -/- ears were used in all experiments. Error bars represent SE. *, indicates p-value of <0.05.

Figure 1.

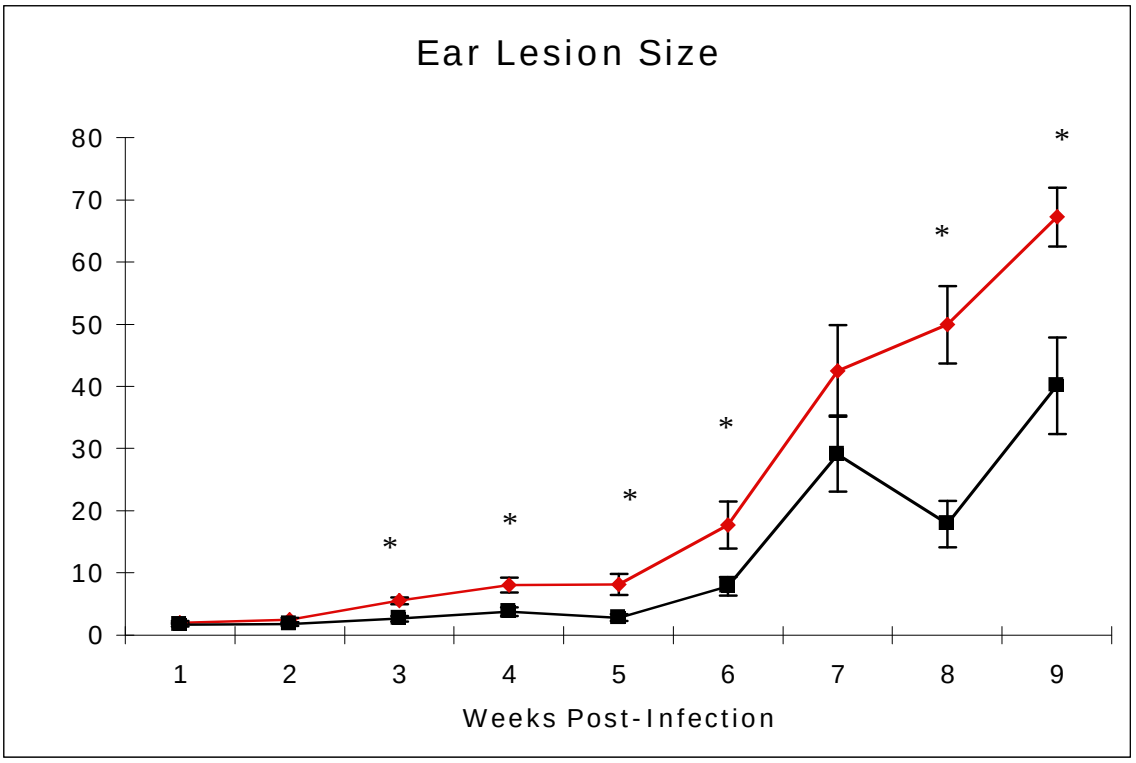


Figure 2.

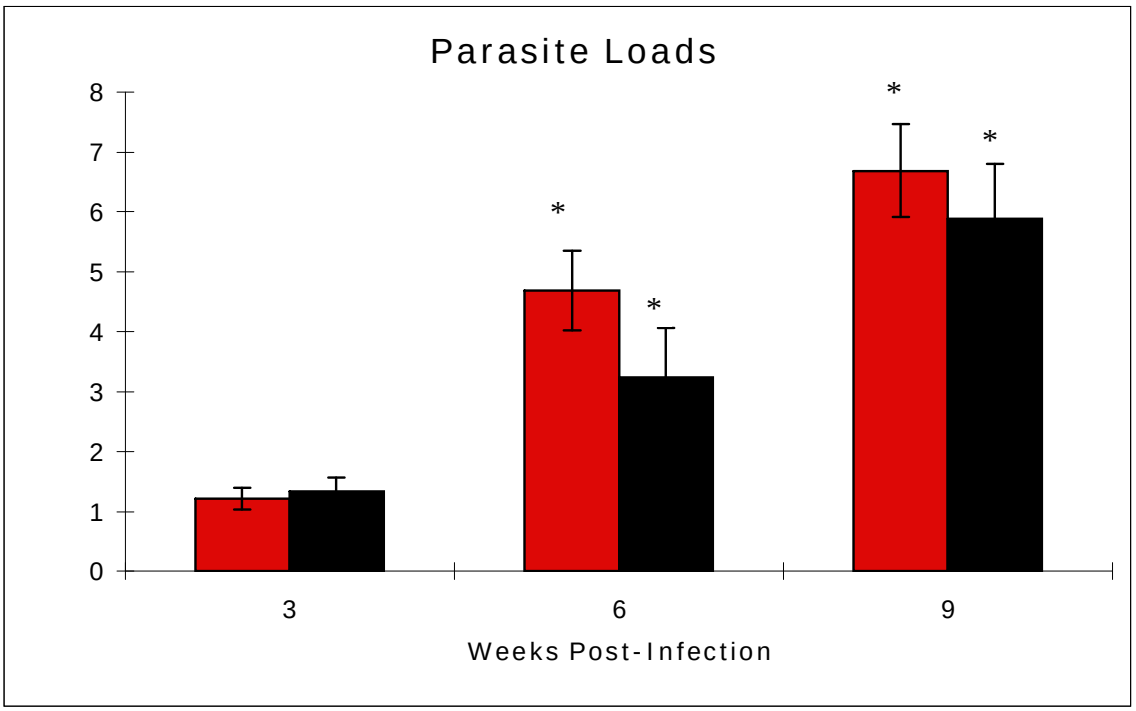


Figure 3A.

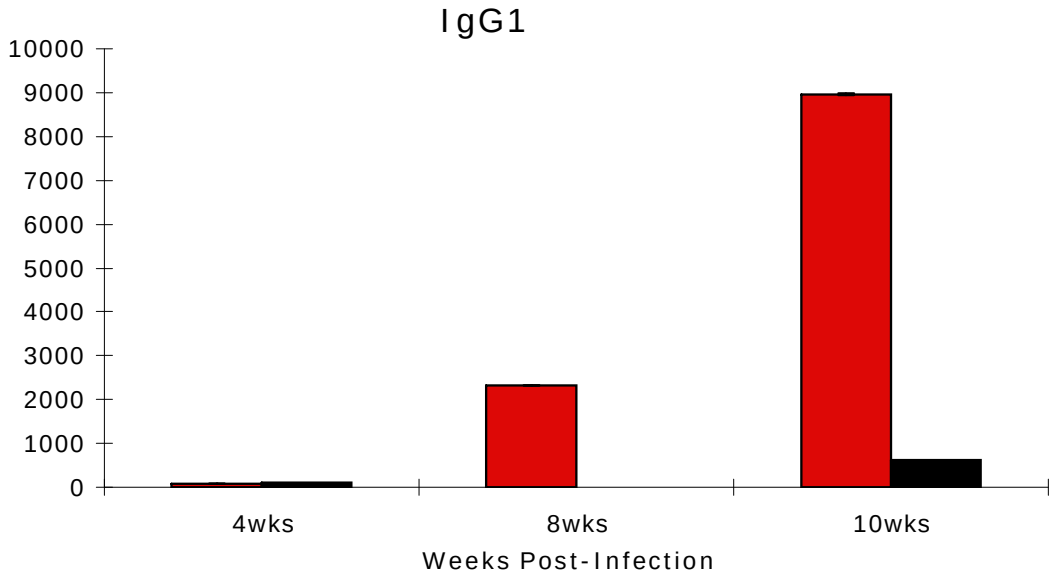


Figure 3B.

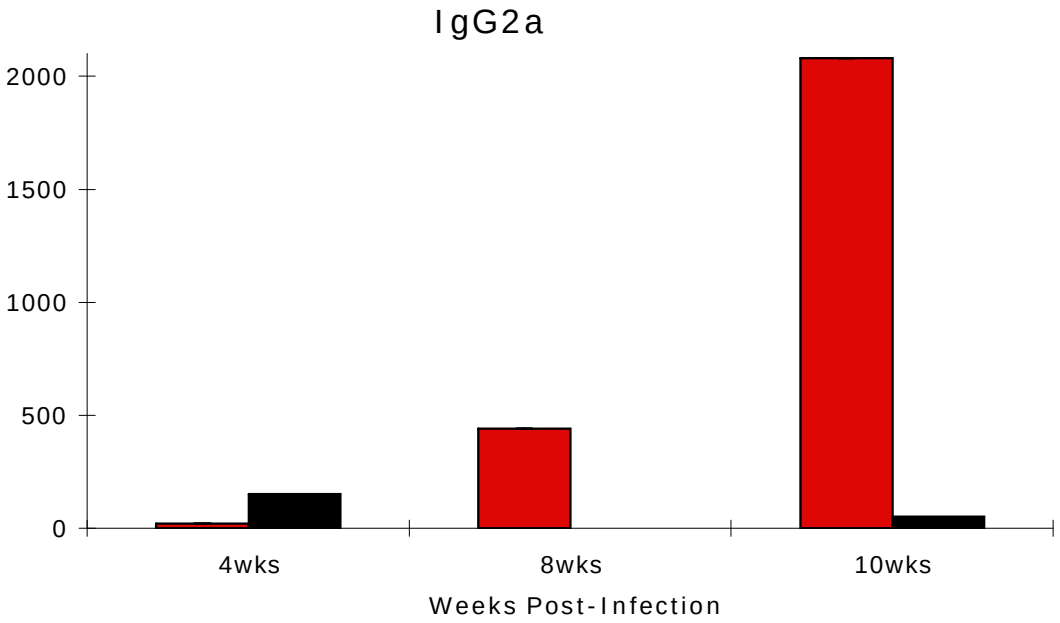


Figure 4A.

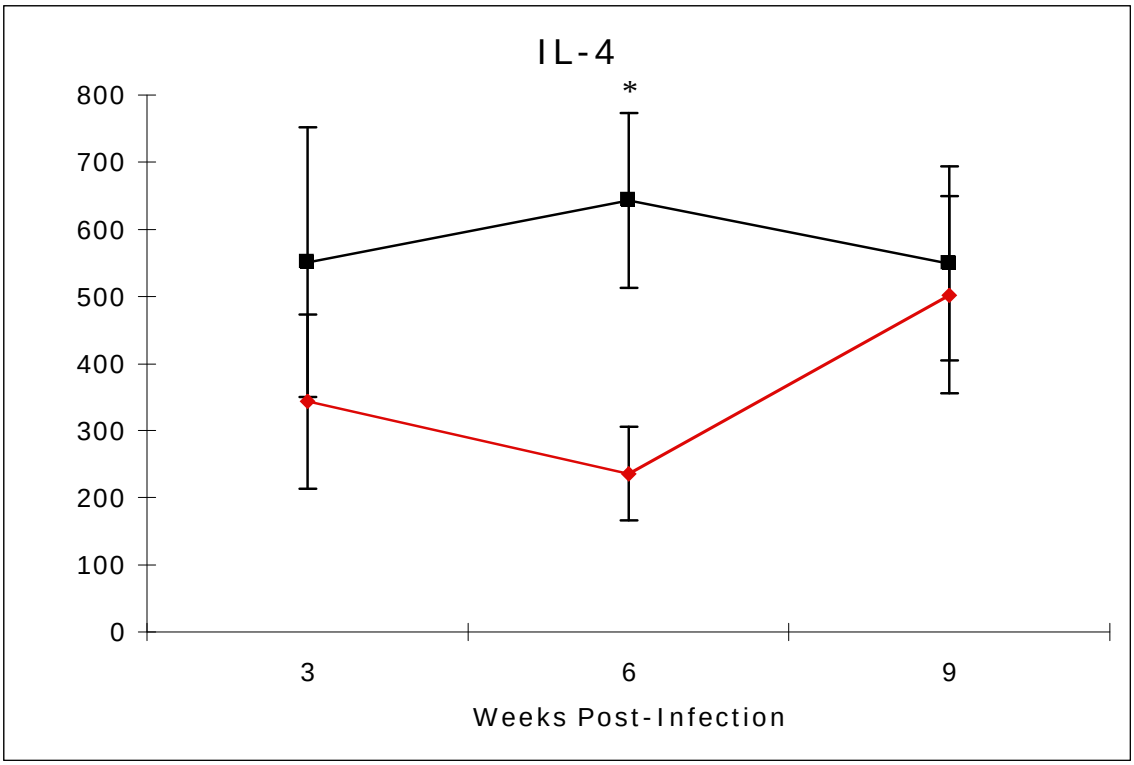


Figure 4B.

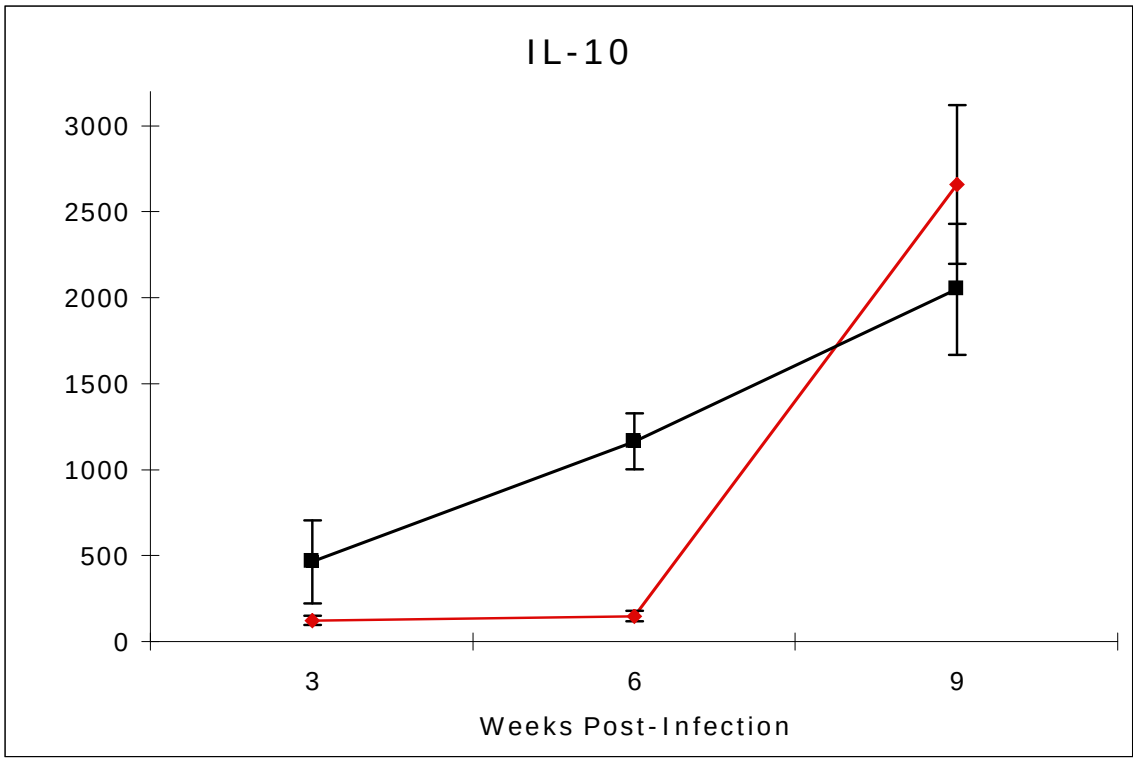


Figure 4C.

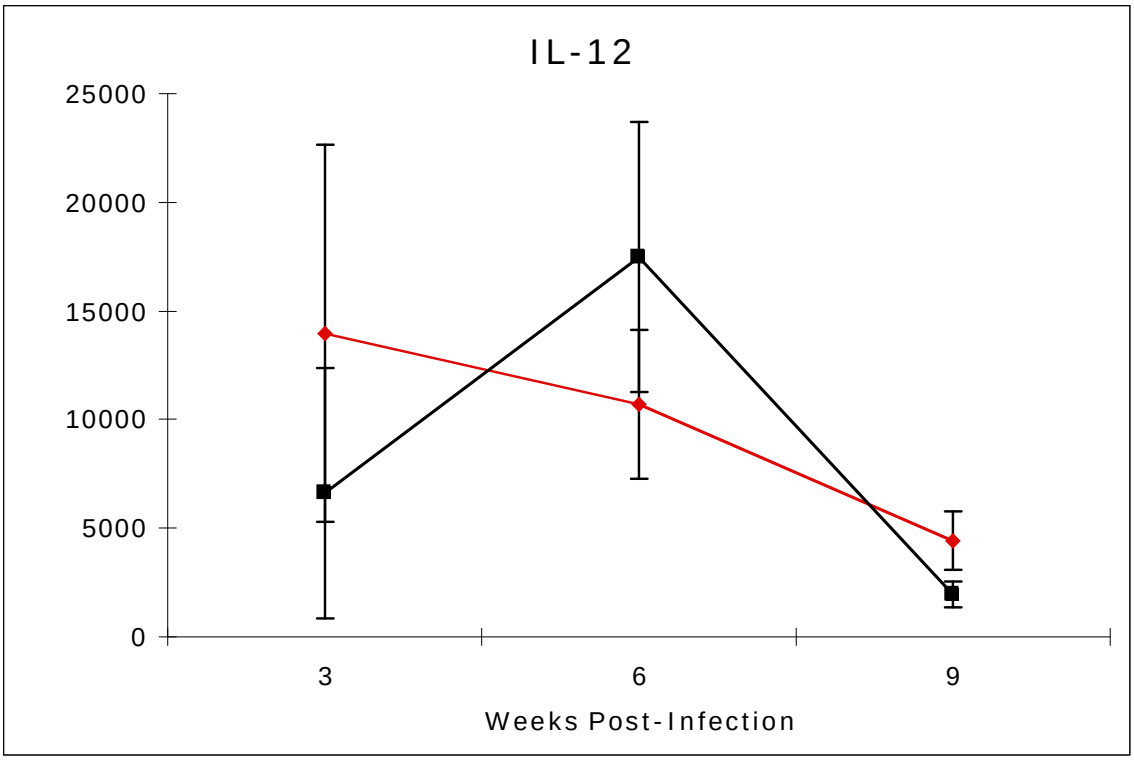


Figure 4D.

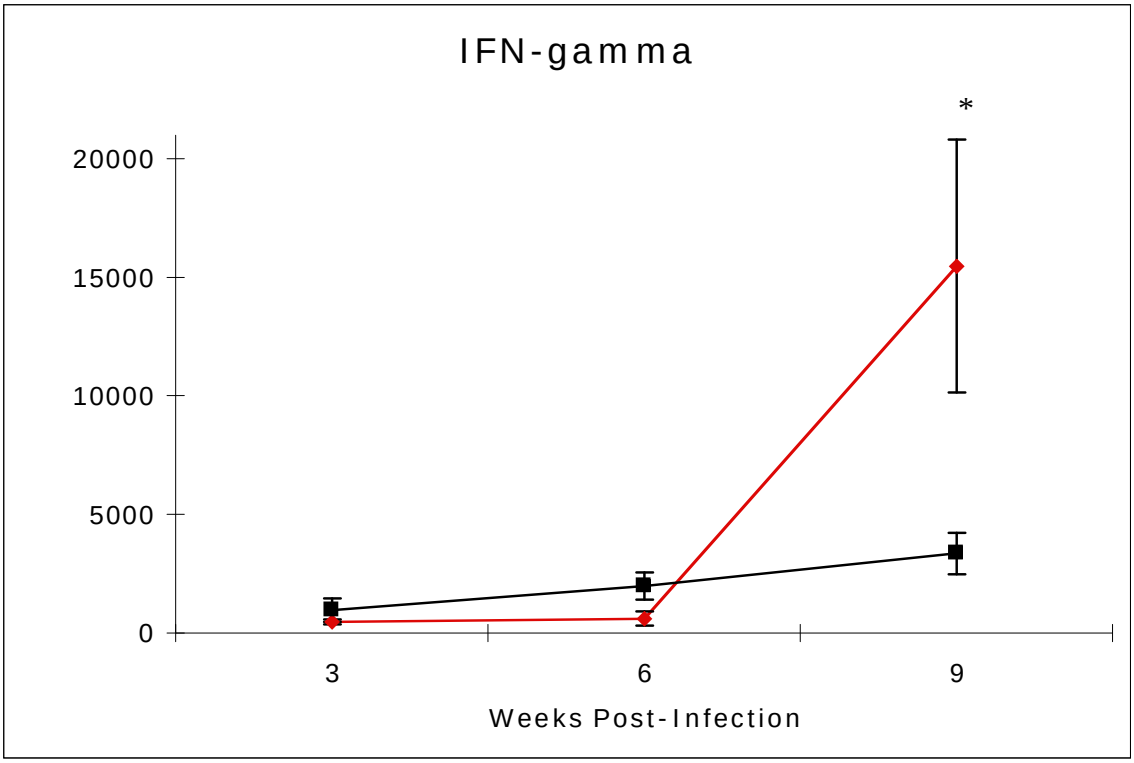


Figure 5A.

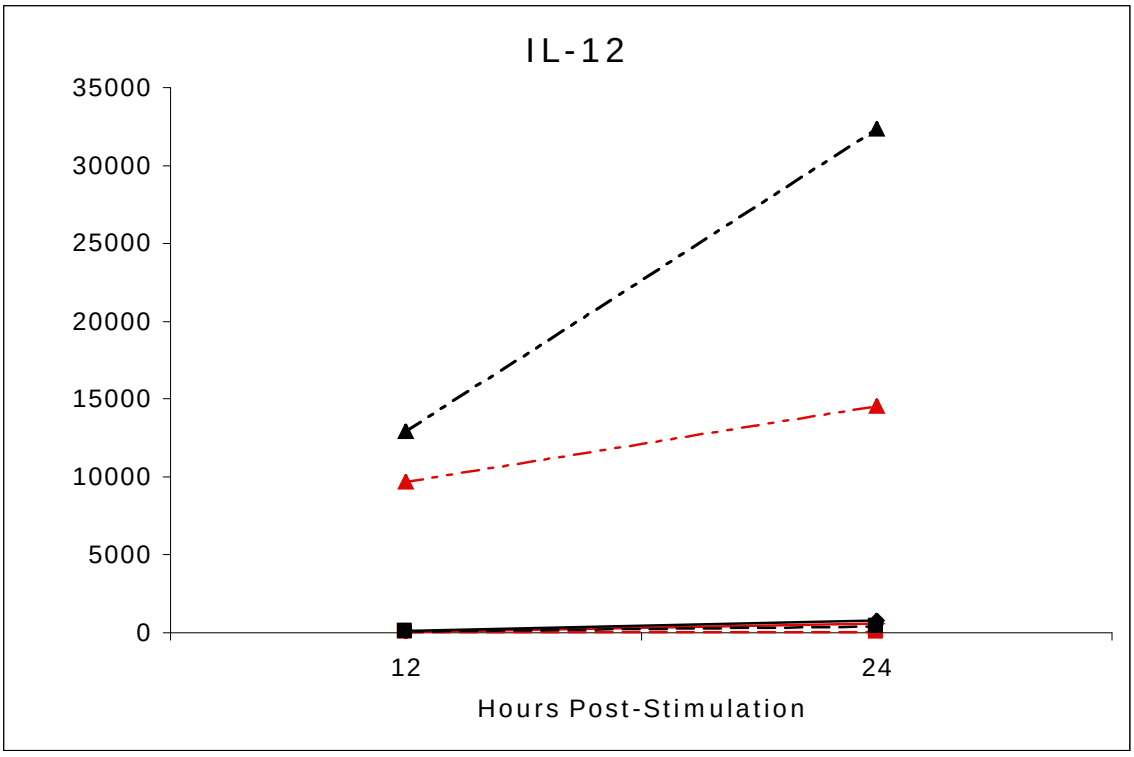


Figure 5B.

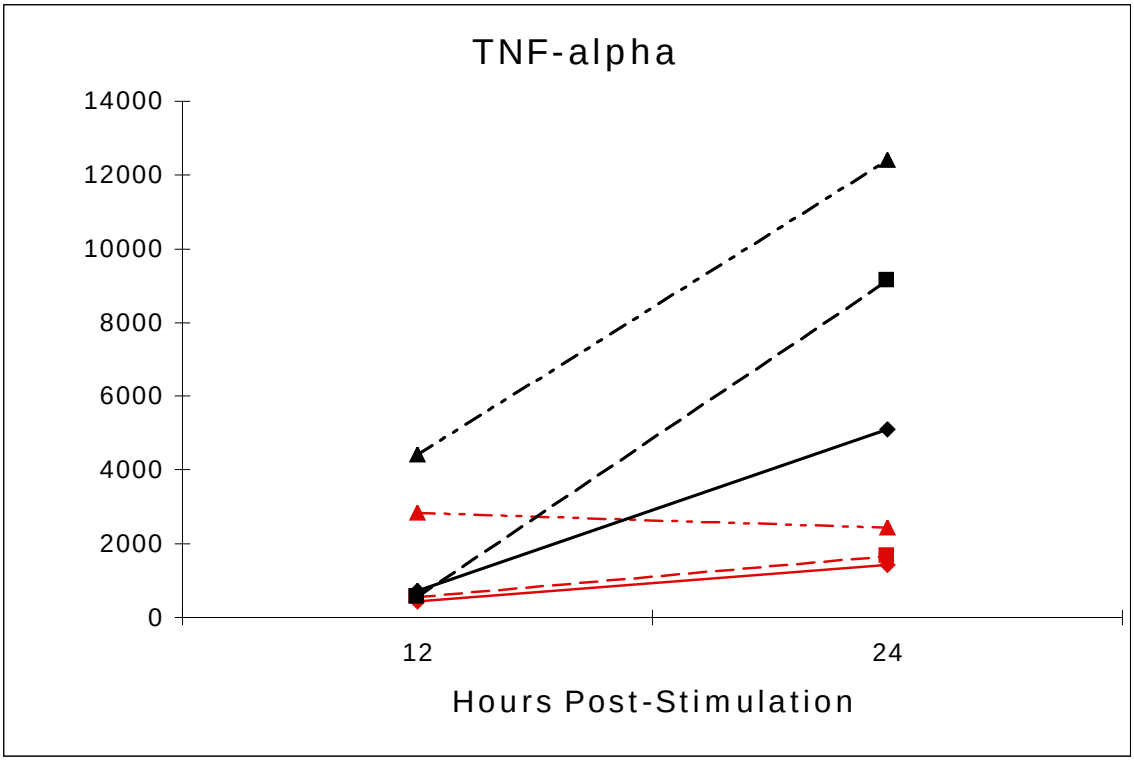


Figure 5C.

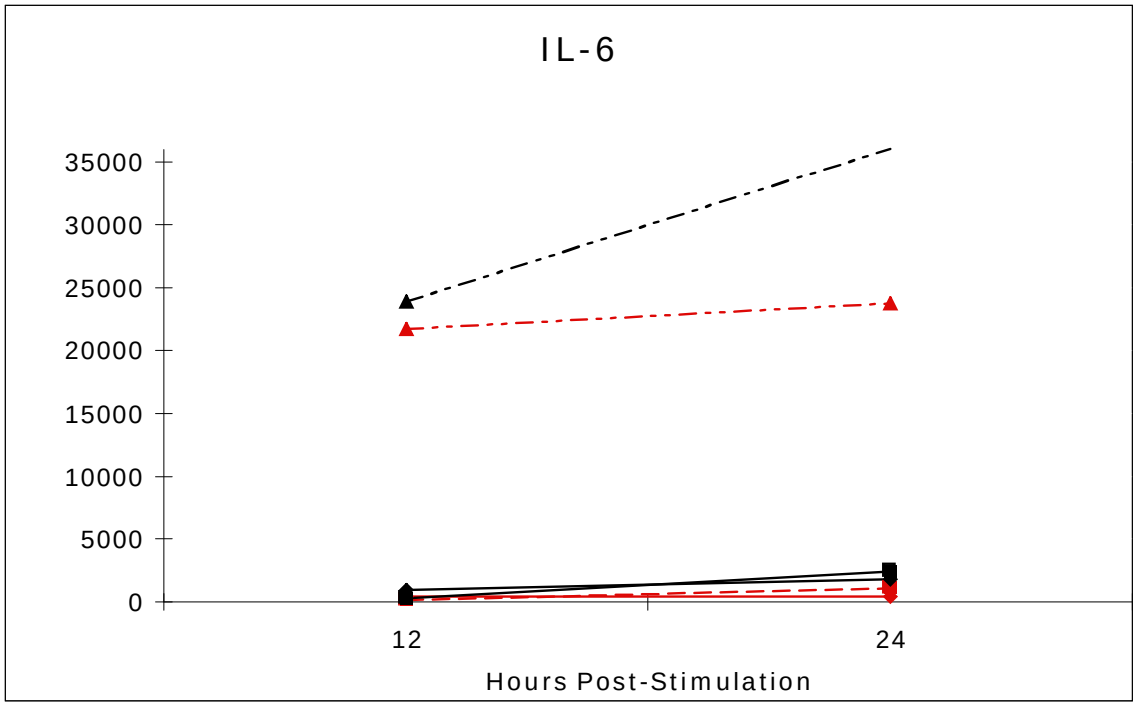


Figure 5D.

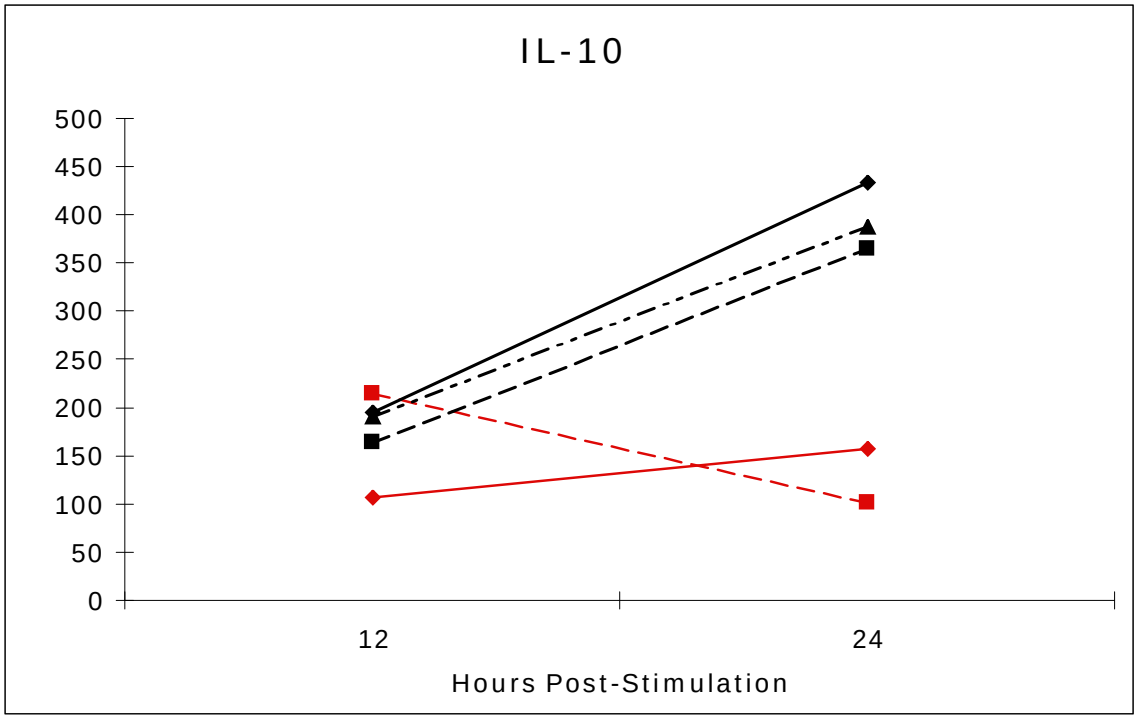


Figure 6A.

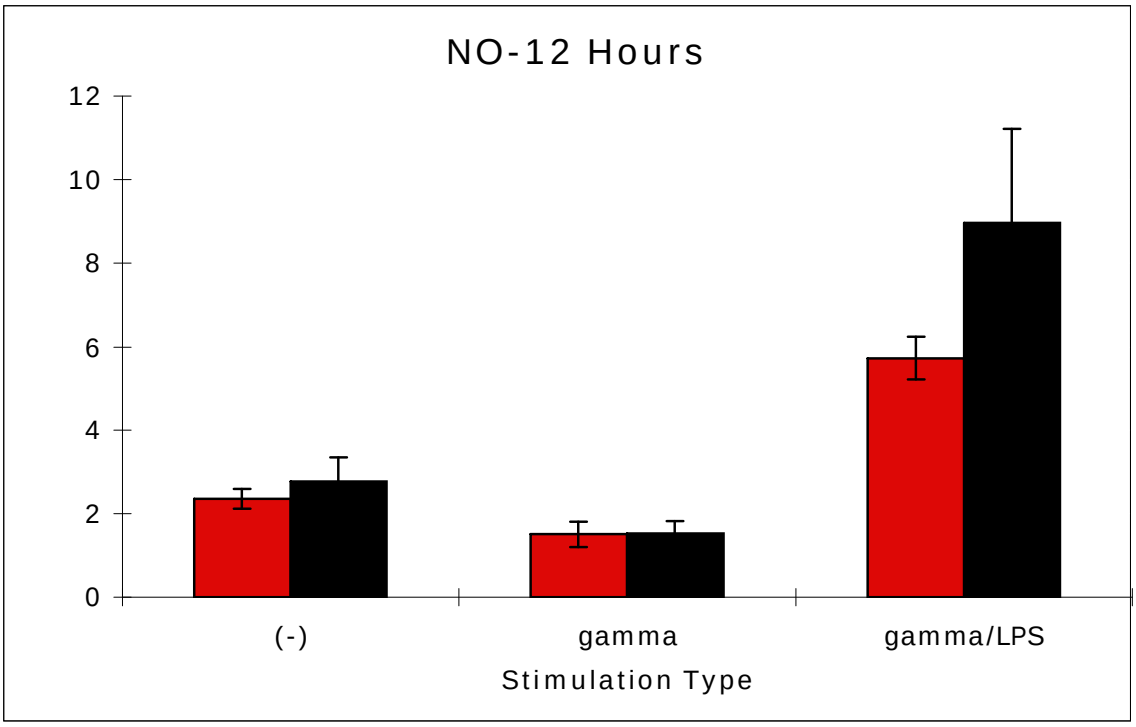


Figure 6B.

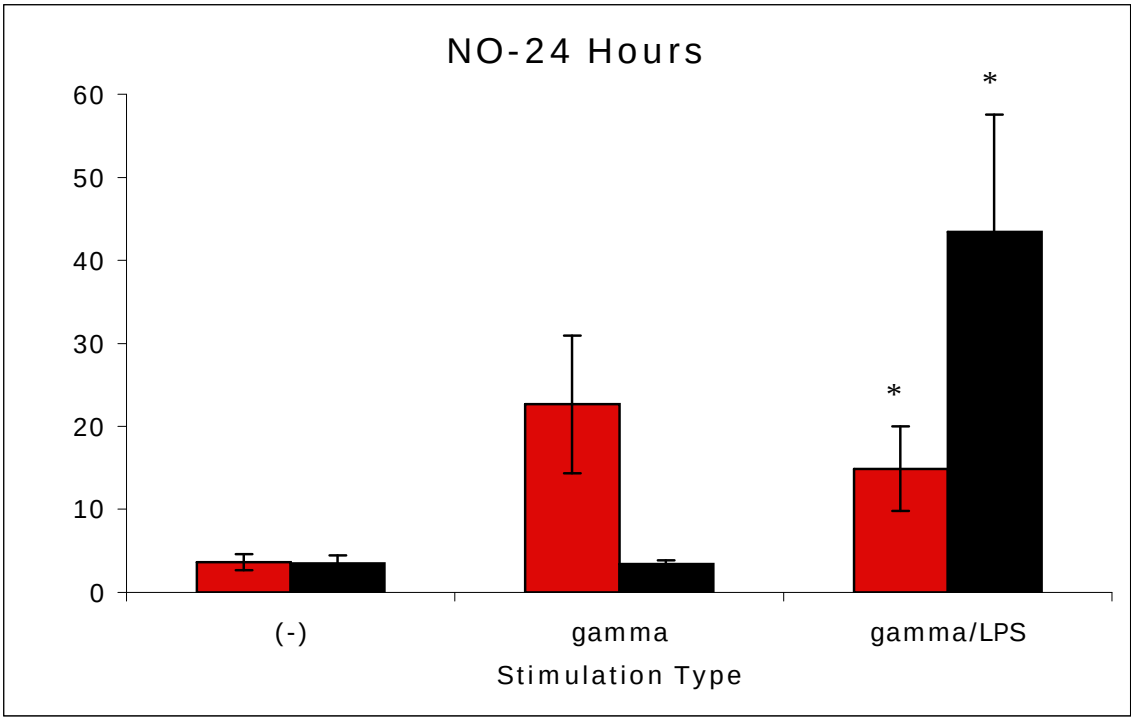


Figure 7A.

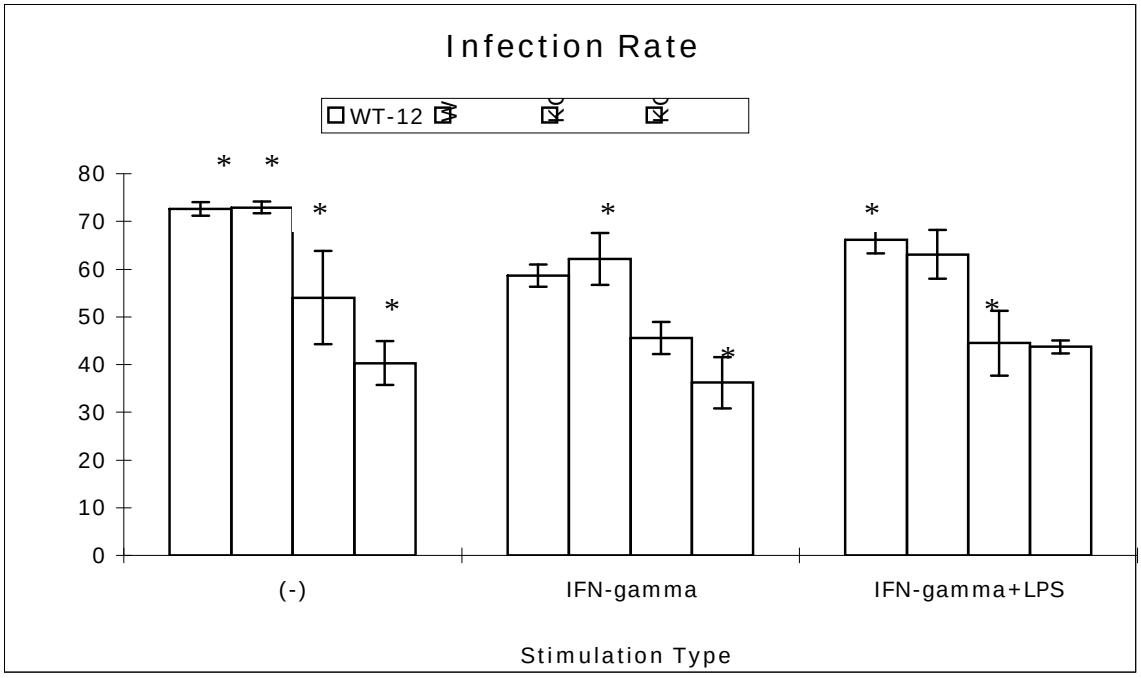


Figure 7B.

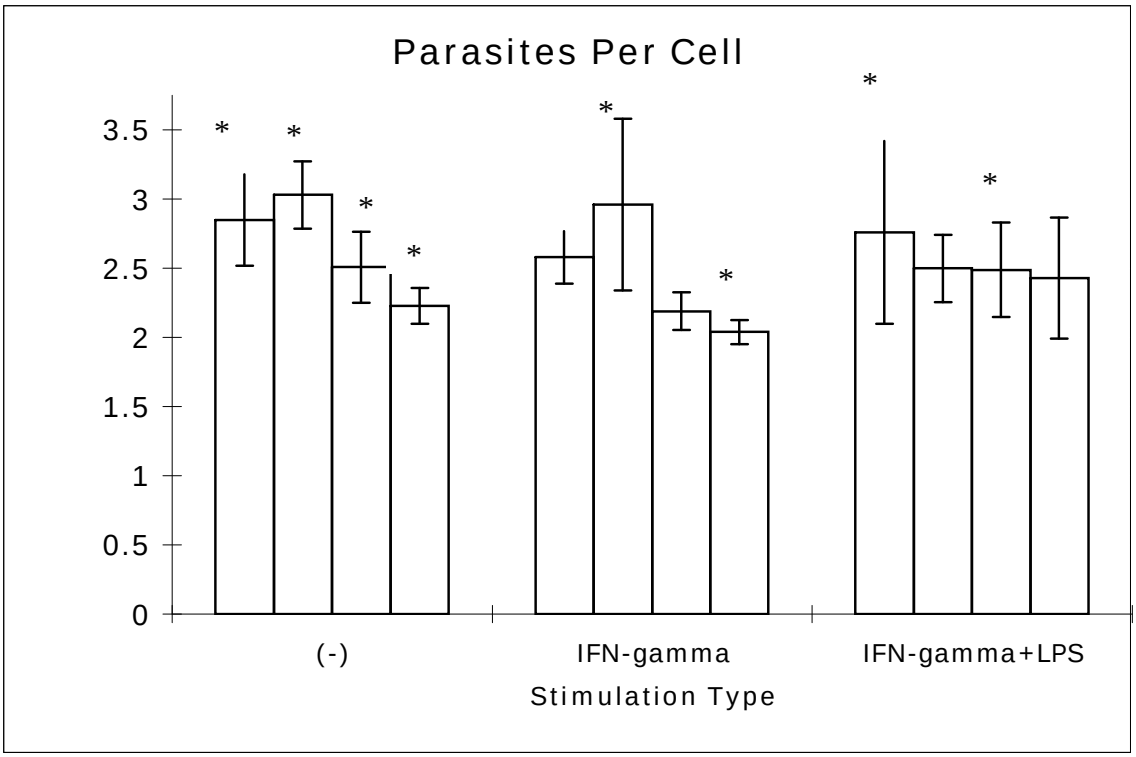


Figure 8.

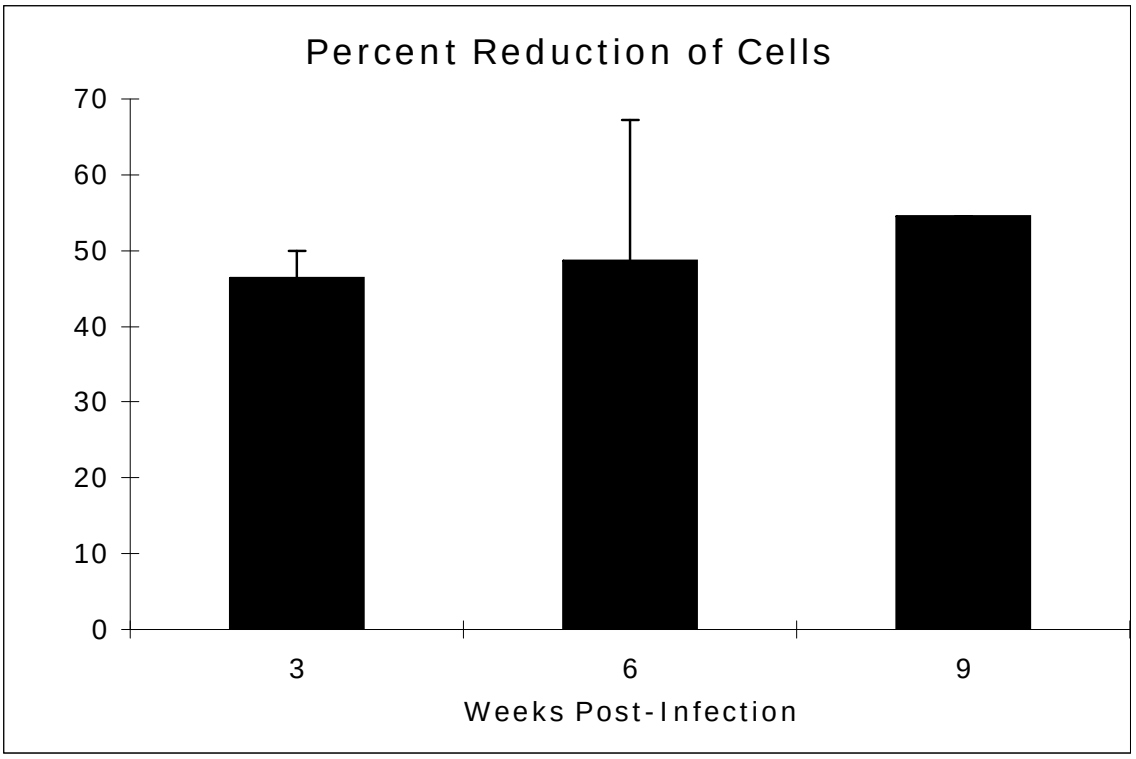
Percent Reduction of Cells
70
60
50
40
30
20
10
0
3
6
9
Weeks Post-Infection